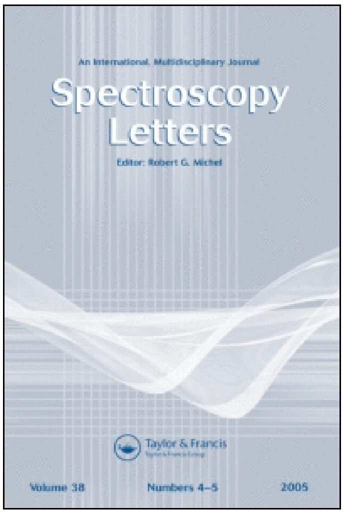

Spectroscopy Letters
Publication details, including instructions for authors and subscription information:
http://www.informaworld.com/smpp/title~content=t713597299

Photon Counting Compression Effects in Pulsed Raman Spectroscopy Using ND:YAG Lasers

A. R. B. de Castro[a]
[a] Instituto de Fisica “Gleb Wataghin”, Universidade Estadual de Campinas - UNICAMP - CP 1170, Campinas, SP., Brasil

To cite this Article de Castro, A. R. B.(1978) 'Photon Counting Compression Effects in Pulsed Raman Spectroscopy Using ND:YAG Lasers', Spectroscopy Letters, 11: 3, 173 — 186
To link to this Article: DOI: 10.1080/00387017808067744
URL: http://dx.doi.org/10.1080/00387017808067744

SPECTROSCOPY LETTERS, 11(3), 173-186 (1978)

PHOTON COUNTING COMPRESSION EFFECTS IN PULSED RAMAN SPECTROSCOPY USING Nd:YAG LASERS

A.R.B. de Castro
Instituto de Física "Gleb Wataghin", Universidade Estadual de Campinas - UNICAMP - CP 1170
13.100 Campinas SP. Brasil

Abstract

We discuss saturation effects in gated photon counting, when the width of the laser pulse is several times the width of the individual anode pulses produced by ejection of a single electron at the cathode of a photomultiplier. A simple model is developed to treat the counting statistics and the results are shown to be in good agreement with experimental data. We also comment on the difficulty of establishing contact with previous work, and emphasize the difference in the domain of applicability of each approach.

1. INTRODUCTION

Pulsed laser Raman spectroscopy allows for efficient discrimination against long lived fluorescence of certain systems(1). It is also the only means to perform Raman studies under conditions of high incident power(2,3). Furthermore, in the case of IR Raman spectroscopy with Nd:YAG lasers, it permits essentially complete elimination of laser rod fluorescences which are Rayleigh scattered and obscure the Raman spectra, as illustrated in fig. 1(4). Work with 1.06 μm

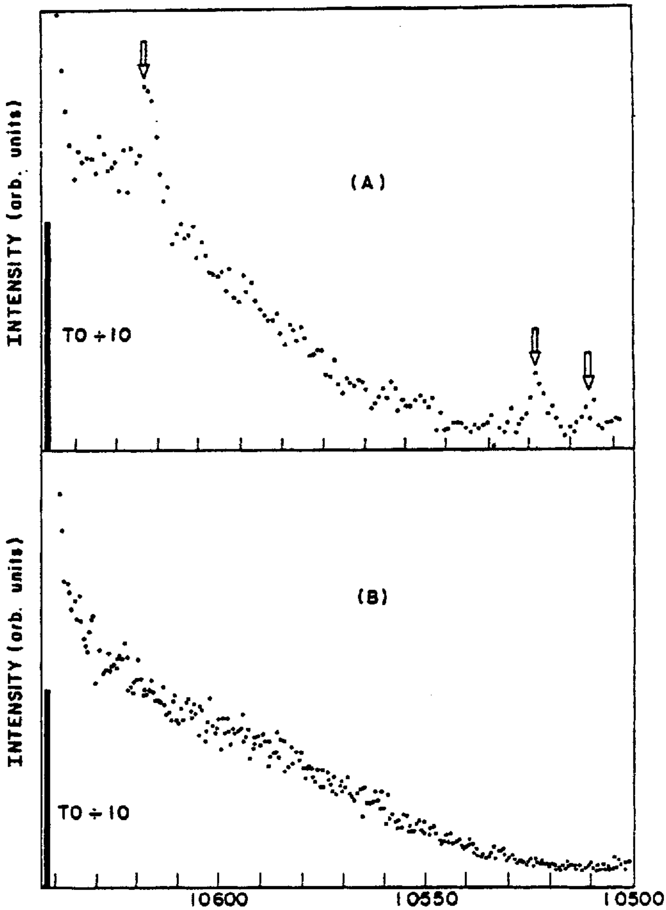

FIG 1 - Single-particle electron scattering in n-doped GaAs. Spectra taken under (A) cw and (B) pulsed excitation with photon counting detection (gated in case (B)). In each case the vertical bar represents the peak intensity of the TO phonon line. Notice the absence from (B) of the three fluorescence peaks indicated in (A).

radiation produced by Nd:YAG lasers (pulsed or cw) is made somewhat difficult by the low sensitivity of the currently available photo-detectors, in spite of developments with negative electron affinity surface technology applied to photo cathodes[(5)].

The low quantum efficiency of the S-1 photo-cathode means that the photomultiplier output current will exhibit wide fluctuations for any given photon flux if the incident light intensity is not high. It is thus desirable to work in the photon counting detection mode.

In this note we discuss photon counting compression effects in pulsed Nd:YAG Raman spectroscopy and show how this can be corrected for. Among other more obvious annoyances this type of saturation can broaden Lorentzian lines in a way that is insidious and not easily detectable because the broadened profile is also Lorentzian.

The situation we want to discuss is qualitatively the following. Each photo-electron ejected at the cathode of a photomultiplier tube generates a current pulse at the anode. The width of this Fast Current Pulse (FCP) depends on the spread of transit times. In the EMI 9684B, for instance, we observed FCP widths in the range from 10 to 20 nsec. By way of comparison, the pulses obtainable from a Q-switched Nd:YAG laser might be 10 to 50 times longer.

Consider the detection of light scattered by a sample on which a laser pulse is incident. During detection there is, at the anode of the photomultiplier tube, a distribution of FCP's.

Their widths, amplitudes and timing fluctuate but their average rate is proportional to the light flux incident on the cathode.

If this flux is very high, the individual FCP's merge to produce a replica of the laser pulse instantaneous intensity. A fast preamplifier-discriminator designed for photon counting sees this anode current as a slowly varying dc level and the counting system registers zero events. This is the extreme saturation limit for photon counting. In this regime Boxcar detection is, of course, highly efficient.

If the light flux is very weak, it is highly improbable to have more than one FCP present at the anode, for each laser pulse.

In this limit the average counting rate is strictly proportional to the light influx.

In the intermediate range (light inputs of moderate intensity) one can have at the anode many resolvable FCP's during a single laser shot. Here we have the possibility of event coincidence and counter dead time effects, which result in a registered count rate lower than the actual number of events per unit time. This is the effect we want to correct for.

For small counting rates, such corrections have been fully discussed by Bédard[6], and more recently by, for instance, Cantor and Teich[7]. The theory developed by these authors is based on Poisson statistics. Insofar as they consider the photoelectric emission process itself, this is clearly adequate. On the other hand, the Poisson distribution is only an approximation when the events considered are the FCP's observed at the anode of a photomultiplier tube. This approximation breaks down when the spacing between FCP's becomes comparable to the width of the FCP. In consequence, even if one defines an effective dead-time taking into account both the width of the FCP and the measured pulse preamplifier/discriminator dead-time, Bédard's theory gives, in the limit of high counting rates, results in disagreement with experiment, as shown in table 1.

2. THEORY

We now replace the actual physical situation described in the previous section with the following soluble model.

Let the counting gate (which might be shorter or longer than the laser pulse - see below) be subdivided into N time intervals of width T. We will call T the effective dead time; this parameter will have to be determined empirically. Upon detection of a laser pulse, some of the N cells shall have been occupied by one or more FCP's. We shall imagine that the

TABLE 1

s	$\overline{k}_E(s)$	$\overline{k}_T(s)$	$\overline{k}_B(s)$
1	1.0±0.1	1.00	.93
2	1.7	1.76	1.72
3	2.2	2.34	2.42
4	2.6	2.75	3.03
5	3.0	3.05	3.57
6	3.3	3.25	4.06
12	-	3.75	6.13

TABLE I - Comparison between theoretical predictions of this work ($\overline{k}_T$), Bédard ($\overline{k}_B$), and experiment ($\overline{k}_E$). The numbers $\overline{k}_E$ were obtained by interpolation of the data displayed in the center of Fig. 3. To calculate the theoretical values we used $(T/\tau)_{\text{Bédard}} = N_{\text{this work}} = 12$; also $(rT)_{\text{Bédard}} = s_{\text{this work}}$.

counter cannot resolve FCP's in a same cell (coincidence of events) nor FCP's in adjacent cells (dead time effect). Then the registered count is given by the number of runs of occupied cells.

We proceed to the evaluation of the average number $\overline{k}$ of sequences of filled cells, given s FCP's to be distributed among N equally probable cells.

The probability P(s,n,N) that n cells be occupied with at least one object, when s objects are distributed among N cells satisfies the following recursion formula:

$$P(s+1,n+1,N) = \frac{N-n}{N} P(s,n,N) + \frac{n+1}{N} P(s,n+1,N) \quad (1)$$

subject to the boundary conditions

$$P(s,n,N) = 0 \quad \text{if} \quad s < n$$
$$P(0,0,N) = 1 \quad (2)$$

Equation (1) results from the following reasoning.

Consider s objects distributed among n or n+1 boxes.

A distribution whereby s+1 objects occupy n+1 cells can be obtained by adding a further object to the collection in one of two mutually exclusive ways. There is a probability

$P_1 = ((N-n)/N)P(s,n,N)$ that the new object occupies one of the N-n boxes still empty. Likewise, there is a probability $P_2 = ((n+1)/N)P(s,n+1,N)$ that the newcomer goes into an occupied box.

The probability P(s,n,N) can also be written in the form

$$P(s,n,N) = f_{sn} N^{-(s-1)} \underbrace{(N-1)(N-2)\ldots\ldots\ldots(N-n+1)}_{(n-1)\text{ factors}} \qquad (3)$$

where the coefficients f_{sn} obey the simpler recursion formula

$$f_{s+1,n+1} = (n+1)f_{s,n+1} + f_{sn} \qquad (4)$$

subject to

$$f_{sn} = 0 \quad \text{if} \quad n>s \qquad (5)$$

$$f_{s1} = 1$$

Given N cells and n filled cells, the probability W(k,n,N) of finding k runs of filled cells is

$$W(k,n,N) = \binom{n-1}{k-1}\binom{N-n+1}{k} \Big/ \binom{N}{n} \qquad (6)$$

as given by Feller[8]. The symbol $\binom{a}{b}$ is the binomial coefficient $a!\,(b!(a-b)!)^{-1}$.

Finally, the average number $\bar{k}(s)$ of sequences of filled cells is

$$\bar{k}(s) = \sum_{n=1}^{s} P(s,n,N) \sum_{k=1}^{n} kW(k,n,N) \qquad (7)$$

We will identify s as the actual average number of events (i.e., FCP's) at the anode, while $\bar{k}(s)$ is the average recorded count rate. In order to correct for coincidence and dead time effects we need to invert (7). This can be done easily (albeit only numerically) by having a computer tabulate $\bar{k}(s)$ as a function of s and N. Table 2 gives the results of such a calculation.

It is empirically found that for large N $\bar{k}/N$ tends to a function of s/N, as might be anticipated on intuitive grounds.

TABLE 2

	N: 4	6	8	10	12	14	16	18	20	22	24
s 1	1.00	1.00	1.00	1.00	1.00	1.00	1.00	1.00	1.00	1.00	1.00
2	1.38	1.56	1.66	1.72	1.76	1.80	1.82	1.84	1.86	1.87	1.88
3	1.47	1.83	2.07	2.22	2.34	2.42	2.49	2.54	2.58	2.62	2.65
4	1.45	1.94	2.30	2.56	2.75	2.90	3.02	3.12	3.20	3.26	3.32
5		1.95	2.42	2.77	3.05	3.27	3.45	3.59	3.71	3.81	3.90
6		1.90	2.45	2.89	3.25	3.54	3.77	3.97	4.13	4.28	4.40
7			2.42	2.94	3.37	3.72	4.02	4.27	4.48	4.67	4.82
8			2.36	2.93	3.43	3.85	4.20	4.50	4.76	4.99	5.19
9				2.89	3.44	3.91	4.32	4.68	4.98	5.25	5.49
10				2.82	3.41	3.94	4.40	4.80	5.15	5.46	5.74
11					3.36	3.93	4.43	4.88	5.28	5.63	5.94
12					3.29	3.89	4.43	4.92	5.36	5.75	6.11
13						3.83	4.41	4.93	5.41	5.84	6.23
14						3.75	4.36	4.92	5.43	5.90	6.32
15							4.29	4.88	5.43	5.93	6.38
16							4.21	4.83	5.40	5.93	6.42
17								4.76	5.36	5.91	6.43
18								4.68	5.30	5.88	6.42
19									5.23	5.83	6.40
20									5.14	5.77	6.36
21										5.69	6.30
22										5.61	6.23
23											6.16
24											6.07

TABLE 2 - Values of $\overline{k}(s,N)$. See eq. 7.

Fig. 2 is a plot of $\overline{k}/N$ against s/N for N=14 and N=26. Even for these relatively small values of N, the two functions differ by less than 8%.

Also it can be shown analytically that expression (7) implies the usual correction formula[9] for incipient photon

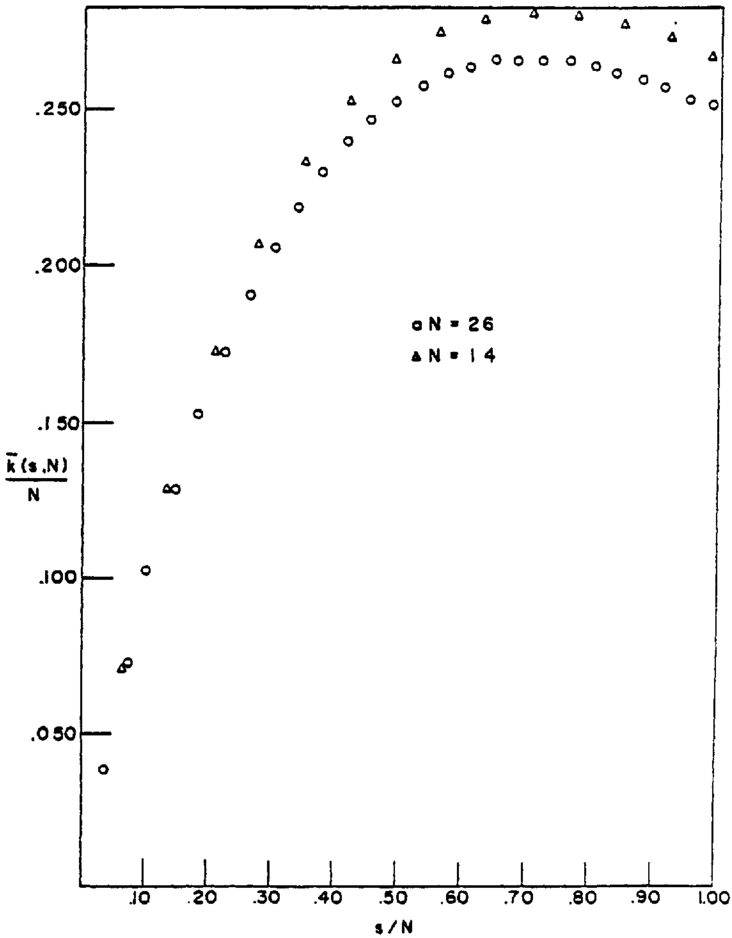

FIG 2 - Plot of $\bar{k}/N$ against s/N for N=14 (triangles) and N=26 (circles)

counting saturation, $f_{actual}=f_{registered}(1-Tf_{registered})^{-1}$ where f_{actual} and $f_{registered}$ are the actual and registered event counting rates respectively.

3. COMPARISON WITH EXPERIMENTAL DATA

In order to compare these theoretical predictions with experiment we counted events at the output of a fast preamplifier/discriminator connected to the anode of the photo-multiplier. The preamplifier was a SSR 1120, with risetime of 6 nsec, 50 Ω input impedance and gain ≥2300. The output was fed into a Tektronix 7D15 200MHz gated counter; the counting gates were provided by a Tektronix 2101 pulse generator.

The counting gate and the output of the preamplifier/discriminator could be simultaneously displayed on a Tektronix 7704A Oscilloscope; this feature makes it much easier to properly adjust the time delay between laser trigger and the opening of the counting gate.

A second pulse generator (Tektronix PG501) triggered both the gate generator and the Q-switch of our Quantronix 112 laser. The average laser output was 1.3 watts, at a laser pulse rate of 1 kHz; the width of the laser pulse was 420 nsec. The experimental setup is shown in figure 3.

The laser beam was focused on a single crystal of GaAs, as for a routine Raman analysis. The scattered radiation was collected at 90° and dispersed by a Spex 1406 double monochromator adjusted for maximum signal at the Stokes transverse optical (TO) phonon line of GaAs.

Figure 4 shows, for various gate widths, the count per laser pulse averaged over 10^5 laser pulses, as a function of photon flux on the photomultiplier detector. The photon flux was varied by inserting calibrated neutral density filters in front of the spectrometer's entrance slit, all other conditions being kept identical. The experimental points correspond to the densities of the filters available to us.

This figure shows, therefore, that under conditions typical of pulsed Raman spectroscopy with 1.06 μm radiation there can be considerable dynamical compression of the signal. The compression is very gradual. The figure also shows that the proposed model is a fair description of the actual physical situation, since a "remapping" of the experimental points with

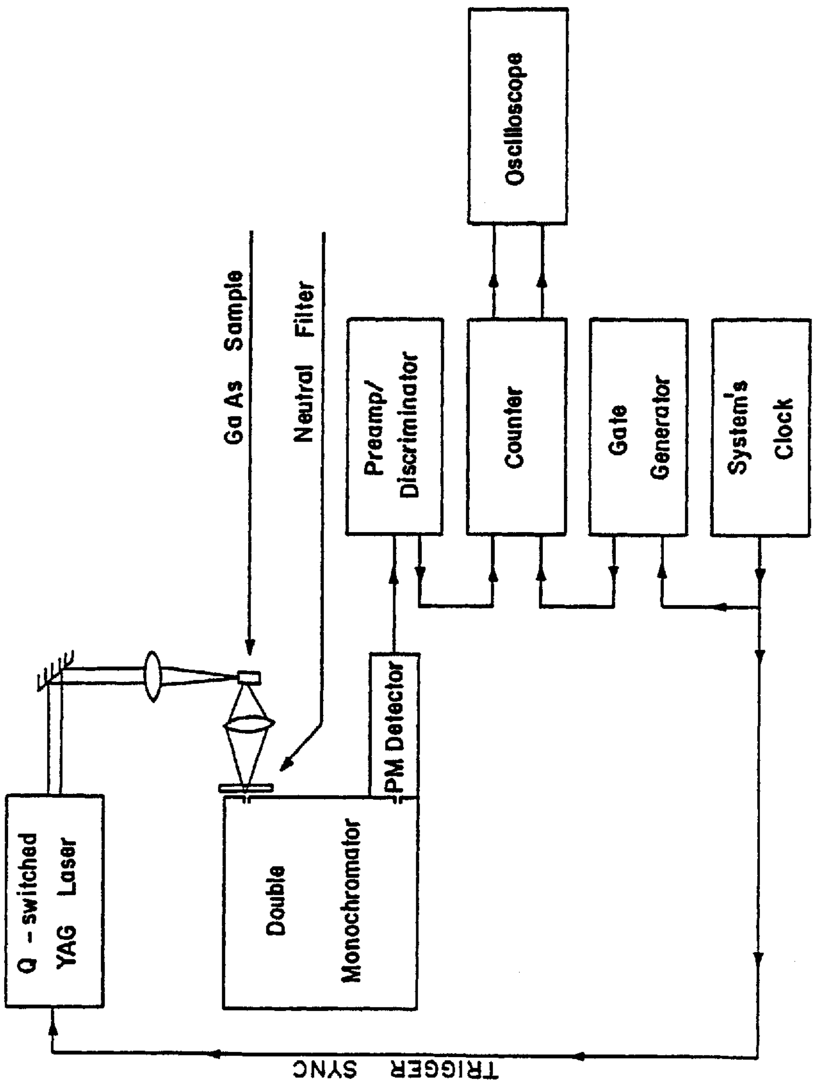

FIG 3 - Diagram of the experimental setup used to gather the data displayed on Figure 4.

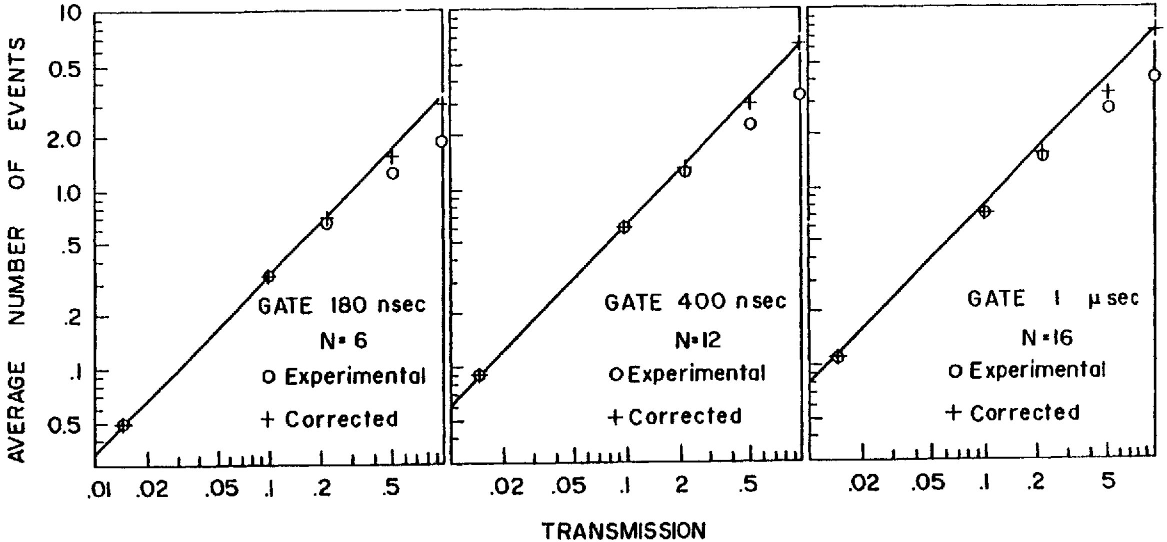

FIG 4 - The circles are the recorded count per laser pulse, averaged over 10^5 laser pulses, as a function of photon flux on the detector. The crosses are the corrected values. Gate width was 180 nsec in (A), 400 nsec in (B) and 1 μsec in (C). We used T=32 nsec in (A) and (B) and chose N=16 in (C).

the help of formula (7) (or rather, its inverse) restores the linearity of the detection system's response.

Although the compression is gradual, it must absolutely be corrected for if linewidth measurements under high intensity pulsed excitation are to be meaningful.

Table 3 shows the spurious broadening of the TO line which results from dynamical compression. In order to obtain these data the Tektronix 7D15 was replaced with a SSR 1110 Counter plus D/A converter and standard chart recorder, gate width being 1 μsec. The Stokes TO phonon line was scanned, with neutral density filters inserted in front of the entrance slit, as explained before.

We now comment on the choice of values for the effective dead time T and the counting gate width. Ideally, the excitation should be zero "outside" and constant during the laser pulses.

The temporal inhomogeneity associated with all real laser pulses is a complicating feature in the analysis we are

TABLE 3.

Filter Transmission	Width (Å)
100%	4.9±0.2
52%	4.2
22%	3.8
10%	3.7
1.46%	3.7

TABLE 3 - Apparent width of TO phonon line in GaAs, as the photon flux at the detector is varied by inserting neutral filters in front of the entrance slit. Light flux on the sample was kept constant.

endeavoring to make. Extra pains were taken in an effort to use gates shorter than the laser pulse width, just to minimize interference from this complicating feature.

The effective dead time T of section 2 must take into account the width of the FCP's and the dead time t of the preamplifier/discriminator. We will define t as the time elapsed between trailing edge of one narrow pulse and leading edge of the next, at the maximum pulse rate the preamplifier/ discriminator will accept.

Both quantities can be measured independently. The FCP-width was estimated by displaying the output of the EMI 9684 B on a fast oscilloscope (additional amplification was provided by a PAR 115 low noise linear preamplifier); the observed average width was 15 nsec. The quantity t was obtained by applying to our SSR 1120 pulses 7nsec wide, increasing the input pulse rate till a decrease in the output pulse rate was noticed, then displaying the input signal on the oscilloscope; this results in t = 17nsec. Accordingly we set T=32nsec.

This assignment results in N=180/32=5.6 and N=400/32=12 for gate widths of 180 nsec and 400 nsec, respectively.

In practice it is frequently convenient to work with counting gates longer than the laser pulse width. When this is the case, the counting aperture is effectively limited by the width of the laser pulse, 400 nsec in our case. However, the best fit is obtained with a T shorter than the value 32 nsec quoted above. What happens is, of course, that saturation may set in at the center of the laser pulse but the wings continue contributing to the signal. Overall saturation is then slower, as if a larger N were applicable. It is expedient in this case to run a "calibration experiment" and determine the effective N directly.

4. CONCLUSIONS

We discussed correction of saturation effects in gated photon counting, when the counting gate is several times longer than the FCP-width . We pointed out some of the deleterious results of such saturation effects and how they can be corrected, on the basis of a simple model.

Levatter, Sandstrom and Lin[10], and Bell and Tyte[11] have also discussed this same problem but in the case of very short excitation (Nitrogen and dye lasers), when the width of the counting gate is equal to the width of the FCP.

It is not clear whether a simple connection can be established between the approach of ref. 10 and 11, and ours. Our discussion is concerned with the statistics of pulse counting at the anode of the photomultiplier tube. If N=1 this statistics is trivial, giving $\bar{k}=0$ or 1. Ref. 10 and 11, on the other hand, stress that when N=1, the statistical process of importance is the light scattering process itself.

ACKNOWLEDGEMENTS

We thank Professor F. Cerdeira and Professor K. Shaklee for critical reading of the manuscript. Financial help from FAPESP, BNDE and CNPq is also gratefully acknowledged.

REFERENCES

1. YANNEY, P.P., J. Opt. Soc. Am., 62, 1297 (1972)
2. LUESMA; E.G., MENDES, G., ARGUELLO, C.A., LEITE, R.C.C., Solid State Com., 14, 1195 (1974)
3. TURTELLI, R.S., de CASTRO, A.R.B., LEITE, R.C.C., Solid State Com., 16, 969 (1975)
4. de CASTRO, A.R.B., and TURTELLI, R.S., unpublished results
5. MARTINELLI, R.U., FISHER, D.G., Proc. IEEE, 62, 1339 (1974)
6. BEDARD, G., Proc. Phys. Soc. (London), 90, 131, (1967)
7. CANTOR, B.J., and TEICH, M.C., J.Opt.Soc.Am. 65, 786 (1975)
8. FELLER, W., "An Introduction to Probability Theory and its Applications", vol. 1 pg. 62 (J.Wiley & Sons, 1968)
9. Instruction Manual of Model 1120 Amplifier/Discriminator, SSR Instruments Co. 1973
10. LEVATTER, J.J., SANDSTROM, R.J., LIN, S., J. Appl. Phys. 44 3273, (1973)
11. BELL, M.J. and TYTE, R.N., Appl. Opt. 13, 1610 (1974)